Epitaxy of Ge Nanowires Grown from Biotemplated Au Nanoparticle Catalysts

Yajaira Sierra-Sastre,[†,*] Shadi A. Dayeh,[§] S. T. Picraux,[§] and Carl A. Batt[‡]

[†]Department of Chemistry and Chemical Biology and, [‡]Department of Food Science, Cornell University, Ithaca, New York 14853, and [§]Center for Integrated Nanotechnologies (CINT), Los Alamos National Laboratory, Los Alamos, New Mexico 87545

ABSTRACT Semiconductor nanowires (NWs) are being actively investigated due to their unique functional properties which result from their quasi-one-dimensional structure. However, control over the crystallographic growth direction, diameter, location, and morphology of high-density NWs is essential to achieve the desirable properties and to integrate these NWs into miniaturized devices. This article presents evidence for the suitability of a biological templated catalyst approach to achieve high-density, epitaxial growth of NWs *via* the vapor−liquid−solid (VLS) mechanism. Bacterial surface−layer protein lattices from *Deinococcus radiodurans* were adsorbed onto germanium substrates of (111), (110), and (100) crystallographic orientations and used to template gold nanoparticles (AuNPs) of different diameters. Orientation-controlled growth of GeNWs was achieved from very small size (5−20 nm) biotemplated AuNP catalysts on all of the substrates studied. Biotemplated GeNWs exhibited improved morphologies, higher densities (NW/μm^2), and more uniform length as compared to GeNWs grown from nontemplated AuNPs on the substrate surfaces. The results offer an integrated overview of the interplay of parameters such as catalyst size, catalyst density, substrate crystallographic orientation, and the presence of the protein template in determining the morphology and growth direction of GeNWs. A comparison between templated and nontemplated growth provides additional insight into the mechanism of VLS growth of biotemplated NWs.

KEYWORDS: biotemplates · S-layer proteins · nanoparticles · nanowires · germanium · vapor−liquid−solid · chemical-vapor-deposition

Interest in nanoscale materials such as semiconductor nanowires (NWs) has been fueled by their unique functional properties and quantum confinement effects that are derived from their quasi-one-dimensional (1D) structure. For instance, the electron−hole binding energy and probability distribution of germanium nanowires (GeNWs) are found to depend on both wire size (*i.e.*, at small diameters) and crystallographic orientation which strongly modify their optical response.[1] Hence, control over the crystallographic growth direction, diameter, and morphology of semiconductor NWs is essential to achieve specific functional properties. In addition, applications of NWs will require precise positioning of high-density NWs in particular configurations and orientations at predefined locations on a substrate. Here, we exploit 2D protein lattices as templates for the assembly of high-density arrays of Au nanoparticles (AuNPs) used in the vapor−liquid−solid (VLS) synthesis of GeNWs.

A VLS process, where presynthesized metallic NPs catalyze the growth of NWs, is an ideal method to control the size of the NWs, as the diameter of the NW is determined by the catalyst size used. However, the poor adhesion of metallic NPs to substrates of technological relevance remains an issue for applications that require very high-density arrays of NWs. To address this issue, substrates functionalized with alkylsilane[2] and poly-L-lysine[3] linkers have been employed to increase the coverage of NPs and have resulted in higher-density growth of NWs as compared to untreated surfaces. However, wire-to-wire spacing cannot be controlled by this approach due to the random distribution of the catalysts on the chemically functionalized substrate surfaces.

Patterning the metal catalysts on the substrate surface provides a means to determine the location of NWs, an important attribute for further device integration. At present, several top-down and bottom-up approaches have been employed for the position-controlled and nanopatterned growth of NWs.[4] Electron-beam lithography (EBL) is the most frequently employed top-down method in the fabrication of Au nanodot arrays for the subsequent catalyzed growth of NWs. While EBL permits fairly high resolution patterning (*i.e.*, ~50 nm features and/or spacings) of metal catalysts, its throughput is slow and not considered suitable for practical manufacturing

*Address correspondence to ys253@cornell.edu.

Received for review November 21, 2009 and accepted January 18, 2010.

Published online February 3, 2010. 10.1021/nn901664r

technologies. Therefore, high-resolution synthetic methods are needed that enable the control of the location, size, and density of NWs. Bottom-up strategies such as mesoporous thin films,[5] nanosphere lithography,[6,7] block copolymers,[8] and porous alumina templates[9−11] have been employed to grow NWs through the patterning of the catalyst on the substrate. An alternative and promising avenue of nanostructured materials research that has achieved substantial development in the last several years involves the use of "natural" macromolecular templates (i.e., biotemplates) with a variety of sophisticated architectures.[12] Biotemplating takes advantage of the structural and physicochemical specificity of biological systems for the assembly of nanoscale materials with complex hierarchies and small dimensions that are difficult to achieve with conventional lithographic techniques.

We have extensively investigated the use of bacterial surface layer (S-layer) proteins as biological scaffolds for the parallel synthesis of ordered arrays of metallic and semiconductor NPs (*e.g.*, Au, Pt, CdSe/ZnS).[13−15] As described elsewhere,[12] S-layer proteins are 2D crystalline arrangements of proteins that constitute the outermost structural component of many bacteria. These structural protein layers are composed of identical subunits ranging in mass from 40 to 200 kDa. S-layers feature a highly repetitive surface structure with nanoscale unit cell dimensions (*i.e.*, 3−30 nm center-to-center spacing). Depending on the bacteria species, S-layers exhibit a variety of different lattice symmetries, including oblique, square, or hexagonal arrays with identical pore dimensions in the 2−8 nm range. The regularly spaced affinity sites defined by the periodic arrangement of identical protein subunits make S-layer lattices particularly suitable for the patterning of nanostructures.[16,17] Stimulated by the extraordinary ability of S-layer proteins to create NP arrays, we have explored the potential of using biotemplated AuNPs to catalyze the growth of NWs. In a recent communication we reported for the first time the VLS growth of high-density, vertically oriented GeNWs of uniform diameters from biotemplated AuNP catalysts.[18] In that work we demonstrated that nucleation and epitaxial vertical growth of GeNWs could be achieved despite the presence of any residual organic "contamination" arising from the S-layer scaffolding.

Here we present evidence of the suitability and compatibility of our biotemplated catalyst approach for the controlled growth of GeNWs from substrates of different crystallographic orientations. Although several reports have addressed the nature of epitaxial growth of GeNWs on crystalline silicon[19,20] and germanium[2,21] substrates, this study demonstrates that orientation-controlled growth of NWs can be achieved from very small sized (5−20 nm) biotemplated AuNP catalysts. Most reported research in GeNW epitaxy has either employed e-beam evaporated gold films[19] or Au colloids (>40 nm)[22] randomly distributed on a clean substrate. Furthermore, we present new insights into the interplay of parameters such as catalyst size, catalyst density, substrate crystallographic orientation, and the protein template in determining the morphology and growth direction of the GeNWs.

RESULTS AND DISCUSSION

Three different catalyst sizes (5, 10, and 20 nm AuNPs) were immobilized on different substrates, that is, Ge(110), Ge(100), and Ge(111), using an hexagonal packed intermediate (HPI) S-layer protein as a scaffold. During GeNW growth, all samples were exposed to the same conditions in a cold-wall, low-pressure chemical vapor deposition reactor using germane as the precursor gas. A standard two-step growth process was used for the GeNW growth, with nucleation of NWs at 370 °C followed by continued NW growth at 280 °C. In all cases, nontapered, highly uniform epitaxial growth was observed from biotemplated Au catalysts. High resolution transmission electron microscopy (HRTEM) imaging showed single crystal NWs with the Au catalyst at the tip and no dislocations or twinning defects for the biotemplated NWs. Furthermore, higher densities and a more consistent out-of-plane morphology were observed with biotemplating. We present below a discussion of the results for the growth of GeNWs for each substrate orientation.

Figure 1 shows scanning electron microscopy (SEM) images of GeNWs grown from biotemplated 5, 10, and 20 nm AuNPs on Ge(110) substrates. The high-density areas of parallel oriented GeNWs as seen from the top-view SEM images (a−c) correspond to NWs grown from AuNPs adsorbed on S-layer protein sheets. The surrounding sparse GeNWs are the background regions where AuNPs adsorbed nonspecifically on the bare substrate surfaces. For all the AuNP sizes, the density of NWs is significantly greater in the biotemplated regions due the effective adsorption of the AuNPs into the vertices of the S-layer proteins.[12,18] Based on their orthographic projection, orientation with respect to the Ge(110) surface, and HRTEM imaging (Figure S1; Supporting Information), the biotemplated GeNWs predominantly grew epitaxially from the substrate along the two available ⟨111⟩ growth directions (Figure S2; Supporting Information).

In the case of NW growth from 20 nm AuNP catalysts (Figure 1c), a high degree of epitaxy was attained in both the background and biotemplated regions with most of the NWs oriented along the ⟨111⟩ direction. For the 5 and 10 nm AuNPs nonspecifically adsorbed at the bare surfaces, there is an increasing amount of GeNWs grown along other orientations (Figure 1a,b). Vertical growth of GeNWs in the [110] direction was also observed for NWs grown from 5 and 10 nm AuNPs (Figure 1d,e). These NWs appear as bright spots in the top view SEM images (Figure 1a,b). As the diameter of the

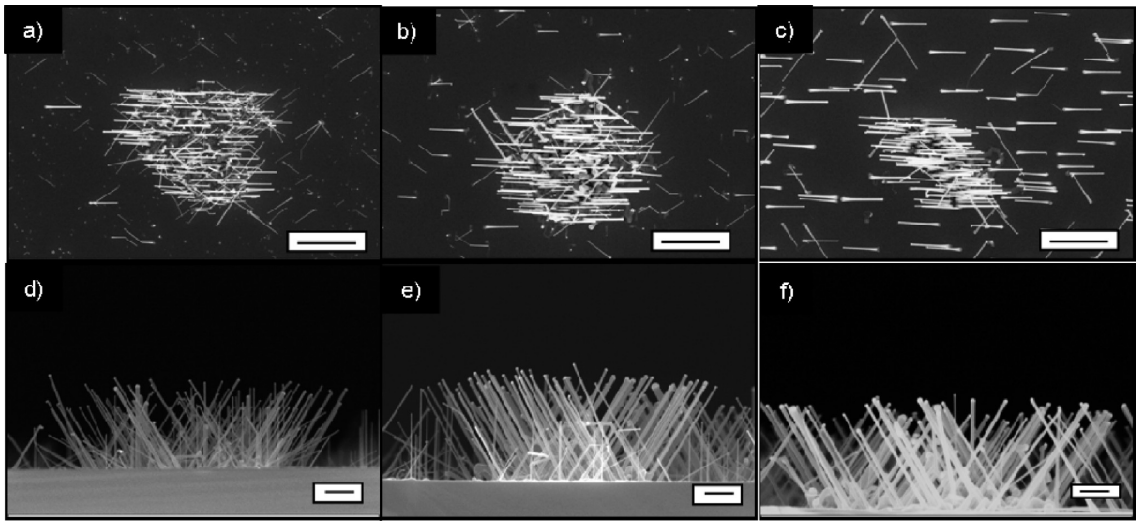

Figure 1. (a−c) Top view and (d−f) cross-sectional view SEM images of Ge nanowires (GeNWs) grown from biotemplated (a, d) 5, (b, e) 10, and (c, f) 20 nm Au nanoparticles on Ge(110) substrates. The biotemplated GeNWs predominantly grow epitaxially from the substrate along the ⟨111⟩ growth directions, which are inclined at 35° to the surface normal in (d−f). Limited vertical GeNWs growth along the [110] direction is also observed. Scale bars: (a−c) 1 μm; (d−f) 200 nm.

AuNP decreases, the number of ⟨110⟩ oriented NWs are observed to increase, particularly for AuNPs that are nonspecifically absorbed outside of the biotemplated regions. This is in accordance with the diameter-dependent growth direction observed by others where nontemplated NWs with diameters <20 nm preferably grow in the ⟨110⟩ direction.[23,24] The increased density of ⟨110⟩ NWs at small diameters is of interest from an electronic perspective owing to the predicted smaller band gap of ⟨110⟩ GeNWs when compared to GeNWs along the ⟨111⟩ and ⟨100⟩ crystallographic orientations at very small diameters.[25]

On the other hand, similar numbers of ⟨111⟩ oriented NWs per unit area grew in the biotemplated regions regardless of the diameter of the AuNP used to catalyze growth (see Table 1). These results contrast with results for GeNWs grown on Ge(111) substrates where the density of vertically oriented NWs increases as the catalyst size increases.[18]

For the biotemplated growth of GeNWs on Ge(100) substrates, two families of NW growth directions were observed. From the top-view SEM images in Figure 2a−c, the NWs of larger diameters correspond to the inclined ⟨111⟩ growth directions. These NWs lie along vertical and horizontal directions in Figure 2a−c, forming rectangular arrays in the plane view. GeNWs of smaller diameters are rotated in projection by an angle of 45° from the ⟨111⟩ oriented NWs, corresponding to the ⟨110⟩ growth direction (Figure S3; Supporting Information). The occurrence of these two growth directions shows a dependence on Au catalyst size consistent with the results for Ge(110) substrates. Figure 3 depicts the relative proportions of NWs for these two different growth directions *versus* the diameter of the AuNP used to catalyze growth. The highest occurrence of ⟨110⟩ GeNWs was observed for NWs grown from 5 nm AuNPs, while the highest occurrence of ⟨111⟩ oriented NWs was observed for the growth of NWs catalyzed with the 20 nm AuNPs. The two growth directions appear to have a crossover at about 10 nm catalyst diameter.

TABLE 1. Biotemplated Catalyst Density (NPs/ μm²) and Ge Nanowire Density (NWs/μm²) as a Function of Catalyst Size and Substrate Orientation

		nanowire density (NWs/μm²)		
catalyst size (nm)	catalyst density (NPs/ μm²)	Ge(111)	Ge(110)	Ge(100)
5	4462	19	14	8
10	1564	30	17	3
20	501	60	16	4

As shown in Table 1, the total GeNW densities achieved for NW growth from biotemplated 5, 10, and 20 nm AuNPs on Ge(100) substrates are significantly lower than for the other Ge substrate orientations studied, particularly for larger diameter NP catalysts. This lower density results from competing AuNP-induced growth along the Ge(100) surface which we now describe. A close inspection within the biotemplated regions in Figure 2 shows the presence of a distinct type of Ge nanostructure growing along the Ge(100) substrate surface. For this orientation ⟨110⟩ growth directions are available in the plane of the (100) surface. These nanostructures, which are sometimes referred to as undergrowth, retain their Au tip (inset Figure 2b) and are linearly oriented along directions perpendicular to one another and in some cases even intersect to form L-shapes. They lie along the two available ⟨110⟩ directions in the plane of the surface and are seen both in the biotemplated and in the background regions (Figure S4; Supporting Information). We propose that these surface nanostructures are prevalent for Ge(100) surfaces because the ⟨110⟩ orientation is a favorable direction for NW growth, and by laying on the surface, there

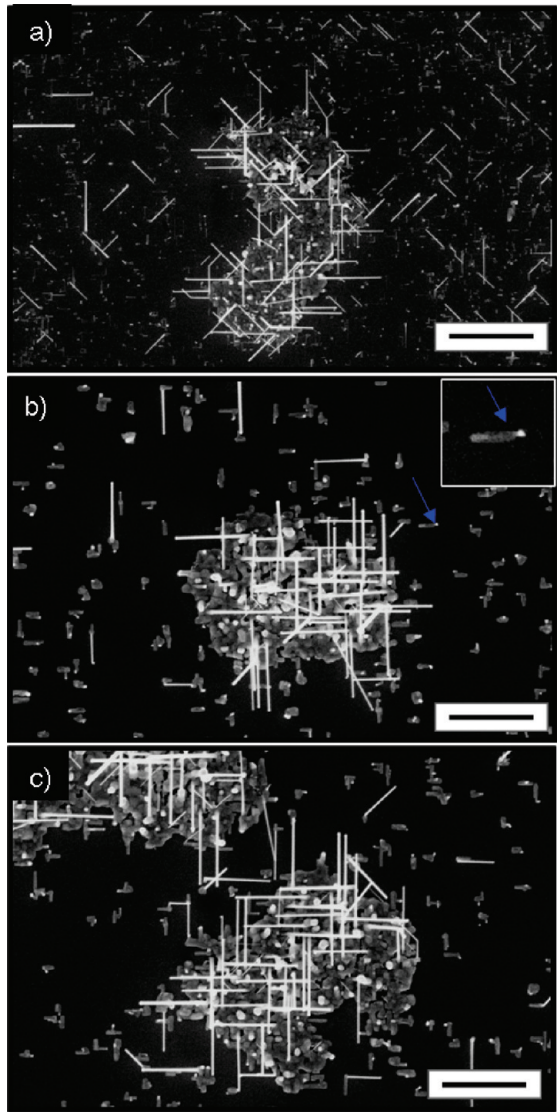

Figure 2. (a−c) Top view SEM images of Ge nanowires grown from biotemplated (a) 5, (b) 10, and (c) 20 nm Au nanoparticles on Ge(100) substrates. Two families of NW growth directions are observed: the ⟨111⟩ (oriented vertical and horizontal in the images) and ⟨110⟩ growth directions (oriented at 45°). Blue arrow in inset (b) points to an isolated nanostructure with a Au tip. These nanostructures grow on the Ge(100) surface along the ⟨110⟩ directions and reduce the density of standing wires in the biotemplated regions. Scale bars: 1 μm.

is a further reduction in the surface energy for the nanostructure. Thus, for the Ge(100) substrate orientation, this undergrowth feature competes with out-of-plane NW growth and reduces the resulting density of standing ⟨111⟩ and ⟨110⟩ NWs.

The results for the growth of GeNWs on Ge(111) substrates are shown in Figure 4. The biotemplated NWs exhibited more uniform morphologies and lengths compared to the GeNWs sparsely grown outside the S-layer templated regions on the substrate surface (Figure 4a−c). HRTEM imaging of a ⟨111⟩ oriented NW (Figure 5) shows very smooth sidewalls and no visible defects for this single crystal, biotemplated VLS growth

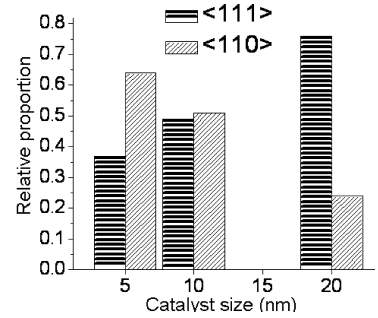

Figure 3. Relative proportions of ⟨110⟩ and ⟨111⟩ growth directions of biotemplated Ge nanowires on Ge(100) substrates as a function of catalyst size. Data collected from five nonoverlapping regions.

approach. Moreover, the vertical [111] epitaxial growth direction was strongly favored (Figure 4d−f) among the available four ⟨111⟩ orientations (the other three orientations are at 55° with respect to the surface normal). This contrasts with the growth on nontemplated regions under identical conditions, where other nonvertical growth orientations were populated.

While orientation-controlled growth of biotemplated GeNWs was achieved for all the substrate crystallographic orientations studied, the highest densities of GeNWs were observed for biotemplated growth on the Ge(111) substrates (see Table 1). Hence, S-layer biotemplating of AuNP catalysts on germanium substrates with (111) crystallographic orientation provides a highly effective parallel approach for the synthesis of high-density, vertically oriented GeNWs. These packing densities are among the highest packing densities reported to date for the seeded growth of GeNWs with AuNPs below 20 nm in size. From a practical point of view, high-density arrays of vertically oriented GeNWs may find applications, for instance, in high-definition terapixel infrared detection[21,26] and rechargeable Li battery systems.[27] From a fundamental standpoint, vertical growth allows the investigation of sample preparation and CVD conditions required to optimize pattern transfer of those biotemplated Au catalyst arrays into that of the synthesized GeNWs, as well as to explore the mechanisms responsible for this improved preferential growth of vertical NWs from biotemplated AuNP catalysts at small diameters.

Recent studies of SiNW growth have shown that Au diffusion from the catalytic AuSi alloy tip occurs at elevated temperatures if the partial pressure of the precursor gas (silane) is reduced during growth.[28,29] As the precursor gas is pumped from the chamber, Au atoms are released from the liquid growth catalyst particle and diffusion on the NW surface results in the formation of small Au clusters along the NW sidewalls and depletion of Au from the tip of the wire. In the present studies the germane gas and heating were shut off simultaneously at the end of the growth run, allowing a short time at elevated temperatures as the susceptor cooled. Scanning transmission electron microscopy (STEM) im-

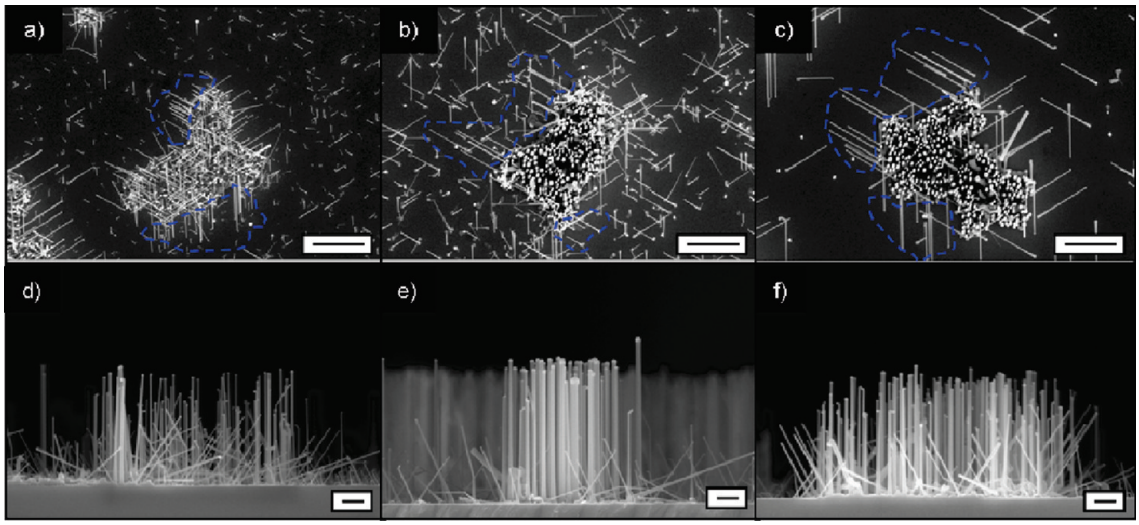

Figure 4. (a−c) Top view and (d−f) cross-sectional view SEM images of Ge nanowires grown from biotemplated (a, d) 5, (b, e) 10, and (c, f) 20 nm Au nanoparticles on Ge(111) substrates. The vertical nanowires are seen as bright spots from the top view images. Inclined wires at the boundaries of the biotemplate are highlighted in blue. Nonvertical ⟨111⟩ orientations exhibit 120° angles in projection. Scale bars: (a−c) 1 μm; (d−f) 200 nm.

aging revealed the formation of small Au clusters along the NW sidewalls and the resultant depletion of the Au catalyst particle. This effect was particularly prevalent for the growth of GeNWs from the smallest AuNPs. It is understood that the AuGe eutectic liquid droplets become less stable with decreasing size due to their increased chemical potential at smaller diameters. This effectively increases the pressure for equilibration with the gas phase which is referred to as the Gibbs−Thomson effect.

In addition, GeNWs grown from the 5 nm AuNPs predominantly showed kinked growth in the nontemplated regions on the Ge(111) substrate as observed by cross-sectional SEM in Figure 6a. Bright-field and dark-field STEM images of a kinked GeNW are presented in Figure 6b,c (also Figure S5; Supporting Information). The observed bright spots in the dark-field image correspond to the Au clusters incorporated along the sidewalls of the NW. The Au at the end of the NW is completely depleted which is expected to terminate the growth of this NW. This effect may explain in part the occurrence of short NWs in the nontemplated regions compared to the NWs in the biotemplated regions. For a different NW of similar diameter, the catalyst droplet volume remained almost constant suggesting that Au migration could be more limited in this case (Figure 6d,e). We speculate that the expected adsorption of contaminants from the organic layer on the catalyst droplets and/or the sidewalls of the NWs could reduce, in part, the diffusion of Au away from the catalyst tip. Kodambaka *et al*. in UHV TEM *in situ* studies have shown that the growth of SiNWs in the presence of a contaminant such as oxygen suppresses Au migration due to the oxidation of the wire surface.[30] In their work, the presence of oxygen during growth led to a lower number density of wires. In our study, the expected adsorption of organic contaminants in the biotemplated regions did not affect the nucleation, morphology, or orientation of the as-grown NWs.

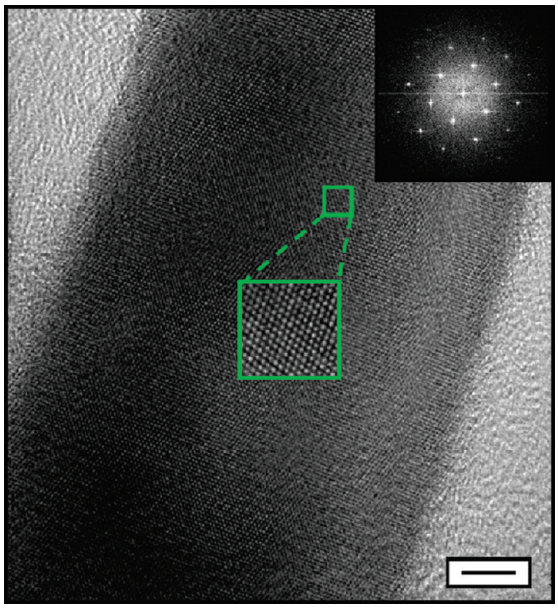

Figure 5. High resolution transmission electron microscopy of a Ge nanowire grown from 20 nm Au catalyst on Ge(111) substrate. The inset highlighted in green shows a magnification of the area. The Fourier transform image (inset) indicates a ⟨111⟩ growth direction; zone axis = ⟨110⟩. Scale bar: 5 nm

As mentioned before, preferential vertical growth of NWs was observed for the growth catalyzed by biotemplated AuNPs on Ge(111) substrates. Figure 7 shows the fraction of vertical GeNWs (green) grown from biotemplated and nontemplated catalyst regions on Ge(111) substrates. In both cases, the increase in the percentage of vertical GeNWs with an increase in catalyst size shows a dependence of vertical growth direction with NW diameter. However, the consistently

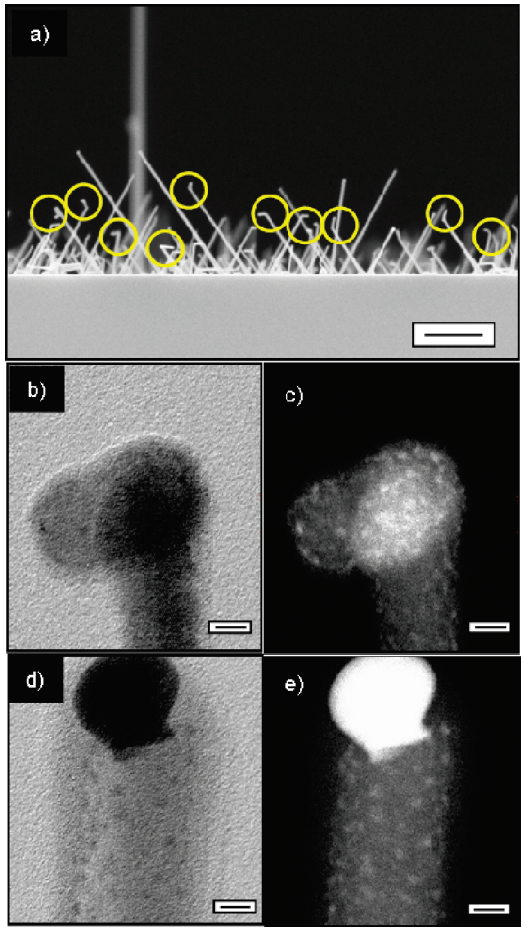

Figure 6. (a) Cross-sectional SEM image of kinked Ge nanowires (yellow circles) grown from nontemplated 5 nm Au nanoparticles at the bare regions of the Ge(111) substrates. (b,d) Bright-field and (c,e) dark-field STEM images of (b,c) a kinked Ge nanowire where the Au has been depleted from the tip of the nanowire by diffusion down the sidewalls and (d,e) a straight Ge nanowire grown on a Ge(111) substrate where there is partial loss of Au from the nanowire tip by Au diffusion. The bright spots in (c, e) are Au clusters along the nanowire sidewalls. Scale bars: (a) 200 nm; (b−e) 5 nm.

higher percentages of vertical NWs observed in the biotemplated regions for the three catalyst sizes suggest that differences in the surface energy balance between biotemplated and nontemplated regions of the catalysts may account for the selectivity in growth direction. We speculate that the nature of the liquid/solid

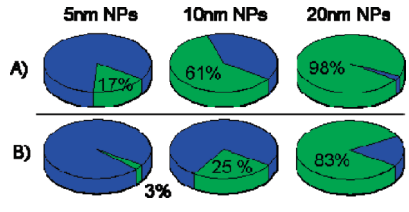

Figure 7. Estimated percentages of vertical Ge nanowires (green) grown from (A) biotemplated nanoparticle (NP) catalysts and (B) nanowires grown from nontemplated NP catalysts adsorbed on bare Ge(111) substrates. The blue sections represent the remained percentages of nonvertical oriented nanowires for each case. The data presented are percentages calculated from three nonoverlapping regions.

interface (*i.e.*, Au/Ge) may contribute to the magnitude of the surface energy balance that defines NW growth direction in the biotemplated regions.

Although we anticipate that the HPI protein monomers denature and decompose at the high temperatures used for NW growth, we presume that any residual carbon layer provides a lateral confining framework that reduces the extent of wetting and spreading of the Au/Ge droplet eutectic on the substrate surface. Imaging of annealed AuNPs provides evidence that supports this assumption. Figure 8a is an SEM image of 10 nm AuNPs after annealing at 370 °C for 5 min, but without GeH_4 flow, clearly showing differences in dimensions between the biotemplated AuNPs and NPs adsorbed at the background regions. Nonspecific adsorbed AuNPs on the bare Ge surface exhibit larger lateral dimensions and lower contrast than those NPs bound to the protein template, indicating a greater degree of interaction with the substrate. We note that such differences between nontemplated and templated regions are not discernible for the larger 20 nm Au catalysts, possibly because of insufficient time for interaction with the substrate in the nontemplated regions (Figure 8b). Additional evidence for this confining framework explanation is given by surface sensitive SEM imaging performed at low energies (1.5 kV) of the incident beam, which provides higher sensitivity to imaging organic layers. As seen in Figure 8d we have observed in some cases the presence of a very thin organic layer with protruding boundaries around the NW base, similar to those seen at the edges of the S-layer protein fragments.

The nonvertical growth of NWs that is generally observed at the boundaries of the protein template (dashed blue regions in Figure 4a−c) also suggests a less effective confinement of the NPs. A surprising aspect of this behavior is that the ⟨111⟩ inclined wires at the boundary of the biotemplated regions seem to not only be away from the interior of the template, but to follow the same growth orientation between neighboring wires (Figure 8c).

The mean diameter values of GeNWs catalyzed with biotemplated 5, 10, and 20 nm AuNPs on Ge(111) substrates were 18, 27, and 38 nm, respectively, that is, 3.7, 2.7, and 1.9 times larger than the original nominal catalyst size used for growth.[31] Annealing experiments during 5 min without growth (no flux of GeH_4 into the CVD chamber) showed that in general, NPs coalescence does not occur even for the smallest biotemplated NPs. We infer that the eutectic formation and melting of AuNPs leading to the coalescence of some NPs does not occur during annealing for short times, but only after the introduction of GeH_4. Consistent with the above discussion, this observation points to a more limited interaction of the AuNPs with the Ge substrate in the templated regions which we have hypothesized is due to the presence of the residual carbon left from the pro-

tein template. Once melting has occurred some coalescence of the closely spaced AuNPs in the templates would be expected. From the GeNW size distributions the susceptibility for Au coalescence increases as the NP size decreases. This is mainly attributed to the small interparticle spacings observed for the biotemplated 5 and 10 nm AuNPs where NPs occupy neighboring vertex points in the protein template.[13]

While many issues remain before S-layer biotemplating of nanoparticle catalysts can produce long-range, ordered arrays of NWs, it is undeniable that the research findings presented herein warrant further study. We envision the exploration of different CVD parameters and mechanisms of growth that will lessen Au coalescence, leading to narrower diameter distributions and patterned growth of NWs.

CONCLUSIONS

In the past several years, an extensive number of reports in the literature have shown the great potential of using biological templates as a bottom-up, synthetic approach for the creation of various arrays of inorganic nanostructures.[12] In the present work, we demonstrated the application of S-layer protein/Au catalyst templates for the successful VLS growth of nontapered GeNWs with uniform diameters and orientations defined by epitaxial growth with the substrate. Orientation-controlled growth of GeNWs from very small sized (5−20 nm) Au nanoparticle catalysts was demonstrated for all major substrate crystallographic orientations, that is, Ge(100), (110), and (111) surfaces. Biotemplated GeNWs exhibited improved morphologies and higher densities (NWs/μm^2) compared to GeNWs grown from nonspecifically adsorbed AuNPs in nontemplated regions of the substrates. Biotemplated GeNWs grew predominantly along the available ⟨111⟩ directions, which is the preferred VLS growth direction, irrespective of the substrate crystallographic orientation. Some vertical growth of GeNWs along the ⟨110⟩ direction was also achieved for the smallest biotemplated catalysts on Ge(110) substrates. For Ge(100) substrates the predominant growth direction changed from ⟨111⟩ to ⟨110⟩ as the AuNP size decreased from 20 to 5 nm, consistent with previous studies for group IV NW growth. Growth on the Ge(111) substrates resulted in a strong preference for ⟨111⟩ NW growth along the vertical [111] direction compared to the growth of GeNWs from nontemplated AuNPs on the substrate. This selectivity in vertical growth is attributed to differences in the nature of the liquid/solid interface and the reduced wetting of the Au/Ge droplet eutectic in the biotemplate compared to the nontemplated regions. The results presented here are relevant to advancing our understanding of the complex interplay of parameters and mechanisms that influence the growth of high-density NWs and the potential use of biological templates for the successful fabrication of these quasi-1D nanostructures.

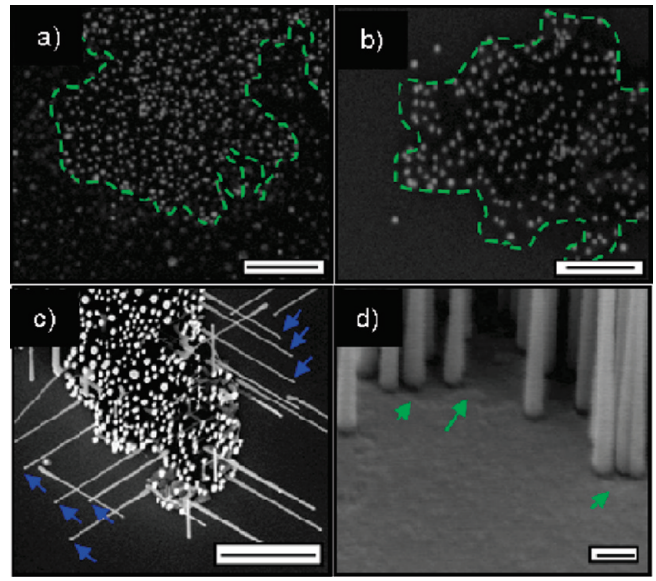

Figure 8. Top view SEM images of (a) 10 and (b) 20 nm annealed Au nanoparticles for 5 min in H_2 without GeH_4 introduction. The green dashed lines highlight the biotemplated regions in (a,b). The nontemplated nanoparticles outside the dashed lines in panel a exhibit less contrast suggesting a greater alloying of the AuNP with Ge substrate atoms. Differences in contrast are not discernible in panel b, indicating a lesser extent of alloying for the large nanoparticles. (c) Top-view SEM image of Ge nanowires grown from biotemplated 20 nm Au nanoparticles. The bright spots are vertically oriented wires. Nonvertical ⟨111⟩ orientations exhibit 120° angles in projection. The inclined wires indicated by the blue arrows tend to follow the same growth orientation at each boundary of the biotemplated region and grow away from the central region of the S-layer. (d) Surface sensitive SEM imaging of the base of the biotemplated NWs shows the presence of an organic layer (green arrows) with protruding boundaries similar to those found in the S-layer fragments. Scale bars: (a,b) 200 nm, (c) 1 μm, (d) 100 nm.

MATERIALS AND METHODS

Cell Culture Conditions and Isolation of S-Layer Proteins. Growth of *D. radiodurans* and extraction of the HPI S-layer fragments were performed as described previously.[18]

Substrate Preparation. The as-received Ge substrates (n-type; Sb-doped) were first sonicated in acetone, isopropyl alcohol, and DI H_2O (5 min each) to dissolve organic contaminants. The substrates were dried with N_2 and further cleaned by ultraviolet (UV) ozone cleaner for 5 min. The Ge substrates were then immersed in DI H_2O for 10 min to dissolve the oxide layer. The substrates were subsequently treated with a 20 wt % HF solution for 10 min to fully hydrogenate the Ge surface and further dried with N_2. The sequential cleaning procedure in hydrogen peroxide, DI H_2O, and HF performed in our previous report was not conducted this time. We observed that in some cases variations in the dipping and rinsing steps caused damage to the substrate surface. Nevertheless, the lack of dipping in H_2O_2 had no effect in the morphology and growth of NWs.

Nanoparticle Patterning on HPI S-Layers. The clean Ge substrates were coated with 10 μL of the HPI stock solution (with their inner face exposed to the aqueous solution) for 45 min at room temperature, and subsequently rinsed with DI H_2O to remove loosely bound HPI sheets. Immediately after the rinsing step, 10 μL of citrate-capped AuNPs (5, 10, 20 nm nominal diameter; Ted Pella, Inc.) were dropped onto the S-layer modified area on the substrate and let sit for 30 min. Finally, the prepared samples

were rinsed in DI H_2O and dried with N_2. The total duration of air exposure between the substrate cleaning and their loading into the CVD reactor was approximately 80 min. Samples were exposed to room light during this period.

Nanowire Growth. The growth was carried out in a cold wall, low pressure chemical vapor deposition system specifically designed for NW synthesis. Sample heating was carried out by a SiC-coated graphite susceptor with a witness thermocouple in the susceptor that was calibrated with a thermocouple-embedded silicon chip to monitor temperature. Prior to growth initiation, samples were heated at 130 °C for 15 min, and subsequently annealed at 370 °C under N_2 (100 sccm) for 12 min. Our rationale in flowing N_2 was to prevent etching of the protein layer and further NP coalescence before nucleation and growth of NWs. We did not find any differences in the epitaxy, morphology, and yield of GeNWs when the samples were annealed either in H_2 or N_2. Therefore, only the results on annealing in N_2 are provided here. A GeH_4 precursor gas (30% in H_2; chamber pressure of 2 Torr, and GeH_4 partial pressure of 0.6 Torr with a flow rate of 250 sccm) was then introduced into the chamber and maintained for 40 s at 370 °C to initiate GeNW growth, after which the temperature was immediately lowered down in 3 min to 270 °C to minimize tapering of the GeNWs during continued growth. The growth time at 270 °C was 5 min.

Microscopy Characterization. Scanning electron microscopy (SEM) of the GeNWs was carried out on a Carl Zeiss SMT Ultra 55 equipped with a thermal field emission source. SEM images of the GeNWs were acquired using short working distances at a low accelerating voltage (WD = 4−6 mm, EHT = 5−10 keV). High resolution and scanning transmission electron microscopy (HR-TEM and STEM) of the GeNWs was performed using a FEI-TECNAI G2 F-20 operated at an accelerating voltage of 200 kV. GeNWs were scrapped with a blade from the Ge substrates and transferred to a carbon-coated TEM grid. A droplet of 2.5 μL of isopropyl alcohol was subsequently added to enhance the adhesion and dispersion of the NWs to the TEM grid surface. Samples were blot-dried using filter paper before imaging.

Acknowledgment. The National Science Foundation (NSF-0403990), U.S. DOE, NNSA, and the Laboratory Directed Research and Development Program at Los Alamos National Laboratory are acknowledged for supporting this work. Y.S.S. also thanks the Cornell Provost Diversity Graduate Fellowship for partial financial support. This work was performed, in part, at the Center for Integrated Nanotechnologies, a U.S. Department of Energy, Office of Basic Energy Sciences user facility, the Cornell Nanoscale Science and Technology Facility (NSF Grant ECS-0335765), and the Microscopy Facility at the Cornell Center for Materials Research (NSF-MRSEC Programs DMR0520404).

Supporting Information Available: (S1, S3) High resolution transmission microscopy images of Ge nanowires grown on Ge(110) and Ge100) substrates; (S2) estimated percentages of ⟨111⟩ oriented nanowires grown on Ge(110) substrates; (S4) SEM image of Ge nanostructures growing along the nontemplated regions on Ge(100) substrates; (S5) STEM images of an Au depleted nanowire tip. This material is available free of charge *via* the Internet at http://pubs.acs.org

REFERENCES AND NOTES

1. Bruno, M.; Palummo, M.; Marini, A.; Del Sole, R.; Olevano, V.; Kholod, A. N.; Ossicini, S. Excitons in Germanium Nanowires: Quantum Confinement, Orientation, and Anisotropy Effects within a First-Principles Approach. *Phys. Rev. B* **2005**, *72*, 153310-1–153310-4.
2. Adhikari, H.; Marshall, A. F.; Chidsey, C. E. D.; McIntyre, P. C. Germanium Nanowire Epitaxy: Shape and Orientation Control. *Nano Lett.* **2006**, *6*, 318–323.
3. Joyce, H. J.; Gao, Q.; Tan, H. H.; Jagadish, C.; Kim, Y.; Zhang, X.; Guo, Y. N.; Zou, J. Twin-Free Uniform Epitaxial GaAs Nanowires Grown by a Two-Temperature Process. *Nano Lett.* **2007**, *7*, 921–926.
4. Fan, H. J.; Werner, P.; Zacharias, M. Semiconductor Nanowires: From Self-Organization to Patterned Growth. *Small* **2006**, *2*, 700–717.
5. Jagannathan, H. D., M.; Nishi, Y.; Kim, H.; Freer, E. M.; Sundstrom, L.; Topuria, T.; Rice, P. M. Templated Germanium Nanowire Synthesis Using Oriented Mesoporous Organosilicate Thin Films. *J. Vac. Sci. Technol., B* **2006**, *24*, 2220–2224.
6. Peng, K. Q.; Zhang, M. L.; Lu, A. J.; Wong, N. B.; Zhang, R. Q.; Lee, S. T. Ordered Silicon Nanowire Arrays *via* Nanosphere Lithography and Metal-Induced Etching. *Appl. Phys. Lett.* **2007**, *90*, 163123163123−3.
7. Fuhrmann, B.; Leipner, H. S.; Hoche, H. R.; Schubert, L.; Werner, P.; Gosele, U. Ordered Arrays of Silicon Nanowires Produced by Nanosphere Lithography and Molecular Beam Epitaxy. *Nano Lett.* **2005**, *5*, 2524–2527.
8. Lu, J. Q.; Yi, S. S. Uniformly Sized Gold Nanoparticles Derived from PS-*b*-P2VP Block Copolymer Templates for the Controllable Synthesis of Si Nanowires. *Langmuir* **2006**, *22*, 3951–3954.
9. Lombardi, I.; Hochbaum, A. I.; Yang, P. D.; Carraro, C.; Maboudian, R. Synthesis of High Density, Size-Controlled Si Nanowire Arrays *via* Porous Anodic Alumina Mask. *Chem. Mater.* **2006**, *18*, 988–991.
10. Polyakov, B.; Daly, B.; Prikulis, J.; Lisauskas, V.; Vengalis, B.; Morris, M. A.; Holmes, J. D.; Erts, D. High-Density Arrays of Germanium Nanowire Photoresistors. *Adv. Mater.* **2006**, *18*, 1812.
11. Erts, D. P., B.; Daly, Brian; Morris, M. A.; Ellingboe, S.; Boland, J.; Holmes, J. D. High Density Germanium Nanowire Assemblies: Contact Challenges and Electrical Characterization. *J. Phys. Chem. B* **2006**, *110*, 820–826.
12. Sotiropoulou, S.; Sierra-Sastre, Y.; Mark, S. S.; Batt, C. A. Biotemplated Nanostructured Materials. *Chem. Mater.* **2008**, *20*, 821–834.
13. Bergkvist, M.; Mark, S. S.; Yang, X.; Angert, E. R.; Batt, C. A. Bionanofabrication of Ordered Nanoparticle Arrays: Effect of Particle Properties and Adsorption Conditions. *J. Phys. Chem. B* **2004**, *108*, 8241–8248.
14. Mark, S. S.; Bergkvist, M.; Yang, X.; Teixeira, L. M.; Bhatnagar, P.; Angert, E. R.; Batt, C. A. Bionanofabrication of Metallic and Semiconductor Nanoparticle Arrays Using S-Layer Protein Lattices with Different Lateral Spacings and Geometries. *Langmuir* **2006**, *22*, 3763–3774.
15. Mark, S. S.; Bergkvist, M.; Yang, X.; Angert, E. R.; Batt, C. A. Self-Assembly of Dendrimer-Encapsulated Nanoparticle Arrays Using 2-D Microbial S-Layer Protein Biotemplates. *Biomacromolecules* **2006**, *7*, 1884–1897.
16. Allred, D. B.; Cheng, A.; Sarikaya, M.; Baneyx, F.; Schwartz, D. T. Three-Dimensional Architecture of Inorganic Nanoarrays Electrodeposited through a Surface-Layer Protein Mask. *Nano Lett.* **2008**, *8*, 1434–1438.
17. Tang, J.; Badelt-Lichtblau, H.; Ebner, A.; Preiner, J.; Kraxberger, B.; Gruber, H. J.; Sleytr, U. B.; Ilk, N.; Hinterdorfer, P. Fabrication of Highly Ordered Gold Nanoparticle Arrays Templated by Crystalline Lattices of Bacterial S-Layer Protein. *ChemPhysChem* **2008**, *9*, 2317–2320.
18. Sierra-Sastre, Y.; Choi, S.; Picraux, S. T.; Batt, C. A. Vertical Growth of Ge Nanowires from Biotemplated Au Nanoparticle Catalysts. *J. Am. Chem. Soc.* **2008**, *130*, 10488–10489.
19. Jagannathan, H.; Deal, M.; Nishi, Y.; Woodruff, J.; Chidsey, C.; McIntyre, P. C. Nature of Germanium Nanowire Heteroepitaxy on Silicon Substrates. *J. Appl. Phys.* **2006**, *100*, 024318024318−10.
20. Dailey, J. W. T., J.; Clement, T.; Smith, D. J.; Drucker, J.; Picraux, S. T. Vapor−Liquid−Solid Growth of Germanium Nanostructures on Silicon. *J. Appl. Phys.* **2004**, *96*, 75567556−12.
21. Nguyen, P.; Ng, H. T.; Meyyappan, M. Growth of Individual Vertical Germanium Nanowires. *Adv. Mater.* **2005**, *17*, 549–553.
22. Woodruff, J. H.; Ratchford, J. B.; Goldthorpe, I. A.; McIntyre, P. C.; Chidsey, C. E. D. Vertically Oriented Germanium Nanowires Grown from Gold Colloids on Silicon Substrates and Subsequent Gold Removal. *Nano Lett.* **2007**, *7*, 1637–1642.

23. Schmidt, V.; Senz, S.; Gosele, U. Diameter-Dependent Growth Direction of Epitaxial Silicon Nanowires. *Nano Lett.* **2005**, *5*, 931–935.
24. Wang, C. X.; Hirano, M.; Hosono, H. Origin of Diameter-Dependent Growth Direction of Silicon Nanowires. *Nano Lett.* **2006**, *6*, 1552–1555.
25. Jing, M. W.; Ni, M.; Song, W.; Lu, J.; Gao, Z. X.; Lai, L.; Mei, W. N.; Yu, D. P.; Ye, H. Q.; Wang, L. Anisotropic and Passivation-Dependent Quantum Confinement Effects in Germanium Nanowires: A Comparison with Silicon Nanowires. *J. Phys. Chem. B* **2006**, *110*, 18332–18337.
26. Yu, B.; Sun, X. H.; Calebotta, G. A.; Dholakia, G. R.; Meyyappan, M. One-Dimensional Germanium Nanowires for Future Electronics. *J. Clust. Sci.* **2006**, *17*, 579–597.
27. Chan, C. K.; Zhang, X. F.; Cui, Y. High Capacity Li Ion Battery Anodes Using Ge Nanowires. *Nano Lett.* **2008**, *8*, 307–309.
28. Den Hertog, M. I. R., J. L.; Dhalluin, F.; Desre, P. J.; Gentile, P.; Ferret, P.; Oehler, F.; Baron, T. Control of Gold Surface Diffusion on Si Nanowires. *Nano Lett.* **2008**, *8*, 1544–1550.
29. Kawashima, T. M., T; Nakagawa, T.; Torii, H.; Saltoh, T.; Komori, K.; Fujii, M. Control of Surface Migration of Gold Particles on Si Nanowires. *Nano Lett.* **2008**, *8*, 362–368.
30. Kodambaka, S.; Hannon, J. B.; Tromp, R. M.; Ross, F. M. Control of Si Nanowire Growth by Oxygen. *Nano Lett.* **2006**, *6*, 1292–1296.
31. The mean diameters of ⟨111⟩ oriented GeNWs catalyzed by biotemplated 5, 10 and 20 nm AuNPs were 17, 22, and 30 nm on Ge(110) substrate and 15, 31, and 36 nm on Ge(100) substrate.